Marian Noga, Akademia Górniczo-Hutnicza, Kraków
Lesław Gołębiowski, Marek Gołębiowski, Damian Mazur
Rzeszów Institute of Technology, Rzeszów

3D FEM MODEL OF THE INDUCTION MACHINE – CALCULATING AXIAL FLUX

MODEL MES 3D MASZYNY INDUKCYJNEJ – OBLICZANIE STRUMIENIA OSIOWEGO

Abstract: A 3D model reflecting entire internal structure of the asynchronous machine using finite elements method, has been presented here. Nodal finite elements have been used to approximate scalar potential and edge finite elements to approximate vector magnetic potential. This model includes both the skew of the rotor bars as well cross current flowing through the rotor iron laminates. The three-phase stator winding is supplied with four-lead mains voltage. The axial flux was calculated by integration of the vector potential around the shaft of the machine. Plots were calculated following the switching on the machine at various speeds. Bar as well as ring fractures were simulated. The simulation results have been confirmed by the theoretical anticipations**.**

1. Introduction

The axial flux in the rotating electric machines is the flux of the vector of the magnetic induction flowing through the plane perpendicular to the axis of the rotor rotation, bounded on the outside by the shadow of the windings, which makes the field forces to align axially. Its major portion flows through the shaft of the machine and then through the bearings. The axial flux is a main flux in the unipolar machines, and in the machines with essentially radial direction of magnetisation, it occurs most frequently due to internal electromagnetic asymmetry of the machine. There are also some phenomena relating to the axial flux in the electric machine. These are e.g. voltages in the motor shaft, which may manifest themselves as current flowing through the shaft and then the machine bearings. These phenomena may also occur due to magnetic asymmetry, as well as capacities found in the machine at supplying with converters. From the electric point of view, the sources, which make them to occur are „perpendicular” to the axial flux stimuli.

Currents flowing through the bearings may lead to bearing failure, and the axial flux may generate eddy currents and bearing heating. This paper will discuss only axial flux.

Finding the correct axial flux is only possible by field calculations, and practically only by 3D FEM. It is useful however to define the prerequisites necessary for developing axial flux in simplified analysis [4], [6]. If axial flux ϕ_u is

due to L – number of facially connected circuits of the elementary machine, i.e. coils and squirrel cage loops,

$$\phi_u \approx c_u \sum_{k=1}^{L} i_k z_k \Lambda_k \qquad (1)$$

The symbols are used as follows:
$i_k z_k$ – ampere-turns of k-th facial connection or current in the squirrel cage sector (including current directions),

$$\Lambda_k = \int_{\gamma_k - \vartheta_k}^{\gamma_k + \vartheta_k} \frac{\mu_0}{\delta_z(\alpha)} d\alpha \quad - \text{ airgap permeance}$$

within the elementary circuit $\gamma_k - \vartheta_k$, $\gamma_k + \vartheta_k$,

$\delta_z(\alpha)$ – substitute airgap attributed to the point located on the circumference of the stator at α coordinate, resulted from the analysis of the magnetic field in the airgap of the machine.
c_u – factor of proportionality depending on the machine dimensions

Thus to develop the axial flux, the

$\sum_{k=1}^{L} i_k z_k \Lambda_k \neq 0$ is prerequisite. One can draw

the following conclusions from this formula:
1) The unipolar flux will be equal to zero once e.g. each facial connection repeats an even number, at equal number of elementary circuits, at positive and negative current direction.

2) Fulfilling the prerequisite formulated in the paragraph 1, but at non-homogeneous air-gap, may make the axial flux to develop.
3) Another conclusion is a notion, that the axial flux level on both sides of the machine might not be equal. Fractured squirrel cage ring on one side of the rotor will make the axial flux to increase on this side of the machine, while leaving some insignificant change on the other.
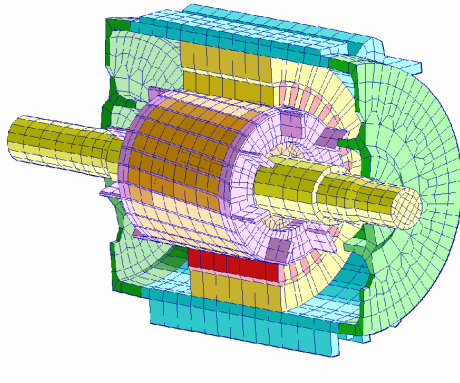

Fig. 1. 3D FEM model of the asynchronous machine

2. 3D FEM model of asynchronous machine

Iron laminates of the machine rotor, was included by magnetic reluctivity tensor of the laminates v. Material conductivity tensor γ was also included. Thus the model includes the cross currents in rotor teeth and yoke, flowing between squirrel cage bars through iron as well as currents in copper in squirrel cage bars and rings. Cubic elements were deformed accordingly to assure correct form of the induction motor. Such procedure appeared to be necessary, as the authors have no procedure for automatic generation of the 3D mesh of finite elements at their disposal. As the 3D modelling requires large number of finite elements, there may be some inconveniences as for the computational speed, and program/computer capabilities, and operating memory usage. These are serious limitations, in spite of that the sparse matrix was used. Thus the cross-sections of non-filleted shape, were assumed. This made it easy to fill the machine elements by cubic elements. Filling the cube elements gaps with tetrahedra that followed acc. to Fig. 2 was easy programming task. This is shown in Fig. 2. It made it possible to include the skew of the rotor squirrel cage bars by selecting appropriately the

magnitude of bar conduction tensor or iron in tetrahedra on the left or right side of the cube [1, 2, 3].
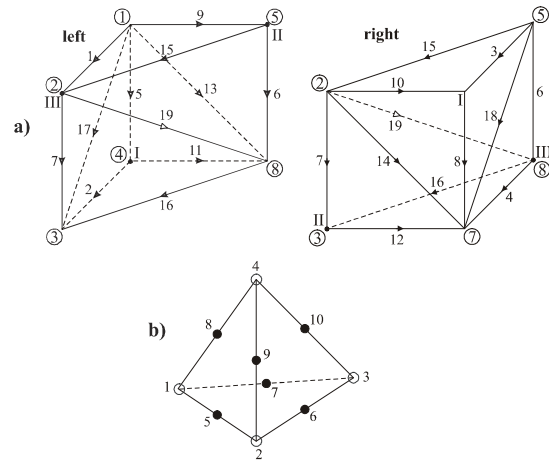

Fig. 2. a) Partitioning of utilised cubic element into 6 tetrahedral elements. b) 2 row approximation of scalar potential in tetrahedron

The rotor shaft, stator and rotor laminates including slots, squirrel cage bars and rings as well as the housing with bearing regions (Fig. 1), were modelled by these finite elements. The 3D model was using vector potential $\vec{A}$ and additionally scalar potential φ in the conducting regions, e.g. laminates, rotor cage bars and rings. The magnetic induction is calculated from the formula of $\vec{B} = rot\vec{A}$. It is assumed that the winding current density of the stator 3 phases, can be expressed by the formula of $\vec{J}_{0i} = rot\vec{T}_{0i}$ introduced additionally for every i-th phase of the vector of $\vec{T}_{0i}$. Thus the equation for the 1st Maxwell law for the non-conducting area $\Omega_{\text{nieprz.}}$ can be expressed as:

$$rot(v \cdot rot\vec{A}) = rot\vec{T}_0, \ where \ \vec{T}_0 = \sum_{i=1}^{3} \vec{T}_{0i}$$

where v is magnetic permeability tensor
For the conductive areas, where eddy currents develop, the following formula is governing,

$$rot\vec{E} = -\frac{d}{dt}\vec{B} = -\frac{d}{dt}rot\vec{A} = rot\left(-\frac{d}{dt}\vec{A}\right).$$

For the purpose of formula generalisation the following relation was included

$$rot\left(grad\left(\frac{d}{dt}\varphi\right)\right) = 0.$$

By omitting rotation operator, the following formula for the eddy current density, induced in

the squirrel cage bars, rings and rotor laminates can be written:

$$rot\vec{E} = -\frac{d}{dt}\vec{B} = -\frac{d}{dt}rot\vec{A} = rot\left(-\frac{d}{dt}\vec{A} - grad\left(\frac{d}{dt}\varphi\right)\right).$$

We are using Ohm's law, which in the conducting continuum of electric conductivity described by tensor of γ binds the current density $\vec{J}$ with electric field intensity $\vec{E}$.

Additionally one has to include the sourcelessness of the current density, $div\vec{J} = 0$ to get the equation system, which describes the electromagnetic field in the machine,

$$\begin{cases} rot(\upsilon \cdot rot\vec{A}) = \vec{J} = \gamma\left(-\frac{d}{dt}\vec{A} - grad\left(\frac{d}{dt}\varphi\right)\right) + rot\vec{T}_0 \\ -div\left[\gamma\left(\frac{d}{dt}\vec{A} + grad\left(\frac{d}{dt}\varphi\right)\right)\right] = 0 \end{cases} \quad (2)$$

To approximate the scalar potential of φ, the tetrahedron local coordinate systems L_i^e, with origins at tetrahedron apices $(i=1,2,3,4)$, which are nodal elements $N_i = \left[L_1^e, L_2^e, L_3^e, L_4^e\right]$, were used. To approximate the vector potential edge finite elements were used. The i-th element of the tetrahedron edge with apices of i_1 and i_2 and of length of l_i, can be written as follows: $\vec{N}_i^e = (L_{i_1}^e \cdot \nabla L_{i_2}^e - L_{i_2}^e \cdot \nabla L_{i_1}^e) \cdot l_i$.

Thus the approximations one can write as:

$$\vec{A} = \sum_i \vec{N}_i \cdot A_i \text{ and } \varphi = \sum_i N_i \cdot \varphi_i.$$

The equations (2) have been brought to weak Galerkin formulation, by multiplying the equations by any variations of the potentials and then by integration along the entire volume of the machine. Linear equation system was solved eventually as:

$$\begin{bmatrix} \nu[R] & 0 & 0 \\ 0 & \nu[R]+\gamma\frac{d}{dt}[C] & \gamma\frac{d}{dt}[D] \\ 0 & \gamma\frac{d}{dt}D^T & \gamma\frac{d}{dt}[G] \end{bmatrix} \cdot \begin{bmatrix} X=\vec{A}\big|_{\gamma=0} \\ X=\vec{A}\big|_{\gamma>0} \\ X=\varphi\big|_{\gamma>0} \end{bmatrix} = \begin{bmatrix} T_0 \\ T_0 \\ 0 \end{bmatrix} \quad (3)$$

where:

$$[R]_{ij} = \iiint_V rot\vec{N}_i \cdot rot\vec{N}_j \, dV; \quad [G]_{ij} = \iiint_V gradN_i \cdot gradN_j \, dV$$

$$[C]_{ij} = \iiint_V \vec{N}_i \cdot \vec{N}_j \, dV; \quad [D]_{ij} = \iiint_V \vec{N}_i \cdot gradN_j \, dV \quad (4)$$

$$[T_0]_{ij} = \iiint_V rot\vec{N}_i \cdot \vec{T}_0 \, dV$$

There is no divergence $div\vec{N}_i = 0$ in the base edge finite elements applied. Thus there is a singular matrix (with zero eigenvalues) in the resulting equation system. A typical equation of such type is the following one, $rot(\nu \cdot rot\vec{A}) = \vec{J}_0$, which is solved by both $\vec{A}$, as well as $\vec{A} + grad\varphi$, at any φ, as $rot(grad\varphi) = 0$. Such equation system can be easily solved by iterative methods, providing that, there are no eigenvectors corresponding to zero eigenvalues of the matrix, found on the right side of the equation system. This condition can be achieved by building the right side of the equation system with the same terms as the matrix of the system. In the case under consideration, these are terms of $rot\vec{N}_i$, for which $div(rot\vec{N}_i) = 0$. This is the reason, which makes it possible to solve the discussed equation system with iterative methods, e.g. with coupled gradients method, minimum residuum method, Chebyshev method, as well as with other methods.

The system of equations (3) is a partial derivative system of independent variables, which are time t and the spatial coordinates x, y, z. The asynchronous machine includes conducting and rotating elements. It is a rotor squirrel cage composed of bars and rings and the laminated rotor stack, which conduct cross currents. Density of eddy currents is expressed by $\vec{J} = \gamma\left(-\frac{d}{dt}\vec{A} - grad\left(\frac{d}{dt}\varphi\right)\right)$. This formula as well as the (3) used the total derivative $\frac{d}{dt}$ in place of partial time derivative of $\frac{\partial}{\partial t}$. This is to underline the fact, that eddy currents follow rotor rotation. The magnetic vector potential $\vec{A}$, as well as the scalar potential φ in these formula, has to be found for the points rotating with rotor. The same symbol ($\frac{d}{dt}$) was preserved also for the conducting stator laminae, although they do not rotate.

There is non-conducting airgap and non-conducting bearings, between fixed stator and rotating rotor. Rotor rotation is simulated by deforming finite elements found in the airgap. On the other hand the finite elements in stator, rotor, shaft and housing are not subject to deformation. The derivative of $\frac{d}{dt}$ („rotating" with rotor) influences only conducting continua, where the finite elements do not deform, so this

derivative does not influence the matrices $[C]$, $[D]$, $[G]$ found in formula (3). They are of constant values. One can say, that this derivative is alternating with these matrices. The applied finite elements method binds the independent variables $[X]$ with mesh, i.e. with the environment and this is where the derivative of $\frac{d}{dt}$ acts upon.

When trying to solve the circuits with coils which are coupled magnetically, as in an asynchronous machine, by using the method described above, one has to consider, that T_0 vector can be written as:

$$\vec{T}_0 = \sum_{j=1}^{f} \vec{T}_j \cdot i_j , \qquad (4a)$$

where i_j stands for current in j-th ($j=1,...,f$; f is the number of stator windings) winding, and $\vec{T}_j$ for the vector corresponding to this winding eg. $\vec{T}_j = \vec{T}_0$, when all the currents, save for the j-th one, equal to zero, and the j-th current is 1A. Then the $\vec{T}_0$ can be transferred from the right to the left side of the equation and new unknowns can be introduced, which are currents. Additional equations are coil voltage expressions,

$$\frac{d}{dt}\Psi_j + R_j \cdot i_j = u_j , \qquad (5)$$

where the flux of Ψ_j is coupled with the j-th winding. This Ψ_j flux can be written as:

$$\Psi_j = \int_V \vec{T}_j \cdot \vec{B} dV = \int_V \vec{T}_j \cdot rot\vec{A} dV ,$$

where $\vec{A} = \sum_{i=1}^{g} A_i \cdot \vec{N}_i$, where g is a number of edge unknowns of vector potentials. It can be seen, that this term appears (with coefficient accuracy) not only in this additional voltage formula, but also in the main equations (3) (once the $\vec{T}_0$ was transferred to the right).

The rotation of the rotor is included by the translation of the nodes located in the machine airgap, and associated tetrahedron deformation. Once the translation equals the tetrahedron edge length, the tetrahedron is brought back to its initial form, but both the nodes and edges at the rotor-to-airgap interface, are renumbered. Three layers of cubes and associated tetrahedra were considered. The torque, as well as the 3 components of the forces acting on the rotor, were calculated by Coulomb method from the layer of tetrahedra adjacent to the stator. The equation system (3, 5) was solved by implicit Crank-Nicholson method [6]. As it includes the values of unknowns and matrices of the system for the final time of integration step, it is a stable method. It is also dictated by the assumed short time step of dt=0,00005 s. In the discussion presented here, a constant rotor speed or its change with time was assumed. If we wanted the program to calculate the speed changes with time, we would need to supplement it by mechanical equations. As the speed changes go much slower than electric processes, this mechanical equation is usually modelled by explicit Euler scheme. Once the discussed numerical methods are applied into the system of equations (3, 5), a large system of linear equations are obtained with sparse matrix. One has to assure the symmetry of system matrix, as it makes it possible to use fast iterations. The majority of iterative procedures of solving linear equations, found in Matlab package, were tested against the computational speed. When applied to larger systems of equations, the procedures from the newer Matlab version, appeared many times slower, than those from older versions. To include the non-linear iron magnetisation characteristic, 3D Newton-Raphson iterative method is usually used. The program presented here was using method of tangents to magnetisation characteristic, also in 3D application. The relation of $\vec{H} = \vec{H}_0 + \upsilon \cdot (\vec{B} - \vec{B}_0)$ was used here, where magnetic intensity $\vec{H}_0$ and magnetic induction $\vec{B}_0$ are the initial values set on the magnetisation characteristic, and magnetic intensity $\vec{H}$ and induction $\vec{B}$ are the values found on the plane tangent to this characteristic. Such relation was substituted in the first equation of the system (2) in place of $\upsilon rot\vec{A}$

The magnetic permeability tensor υ is a symmetric one. The iron magnetisation characteristic was assumed in the form of polynomial of $H=h_1B+h_3B^3+h_9B^9$, where H and B are absolute values of magnetic intensity and magnetic induction in iron respectively. At calculating the υ tensor for each finite element with magnetic non-linearity, it was assumed, that it is composed of laminate separated by non-magnetic insulating layers. The filling ratio of laminated stack was assumed as iron area to entire stack

cross-section. This tensors could be also calculated from energy formulae. In the program discussed here, the Kirchhoff laws were directly applied into the laminated stack. The sparse matrix available in the Matlab package, *COO* type was used to simulate entire problem.

3. Calculation of the transient states by using 3D model of the asynchronous machine

Asynchronous squirrel cage machine was modelled with one pole pair of 12 stator teeth and 14 rotor bars of the such skew which corresponds with 1 slot pitch of the stator.

The results of the numerical simulations are shown in the plots below.
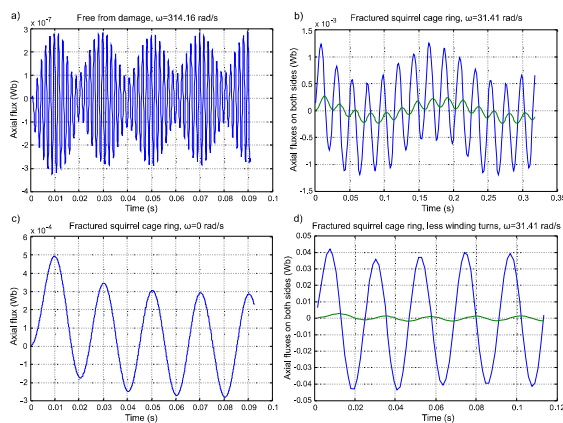
Fig. 3. Axial flux, a) machine free from damage, b,c,d) fractured squirrel cage ring, speed a) ω=314 rad/s, b) ω=31.4 rad/s, c) ω=0, d) ω=31.4 rad/s (less winding turns per phase)

The results shown in Fig. 3a indicate, that axial fluxes in the case of the machine free from damage are insignificant. The Figs. 3b, c, d, corresponding with fractured rotor squirrel cage on the one end of the machine, show marked increasing of these fluxes. Figs. 3b, d show, that axial fluxes increase more prominently on that end which is closer to the damaged region. From Fig. 3 one can find main pulsations of the axial flux versus speed. These pulsations agree well with gauged results and simplified theoretical analysis [5, 8, 9]. They are s ω_0, where s is slip of a machine and ω_0 is supply pulsation (the pole pair number p of the machine is 1).
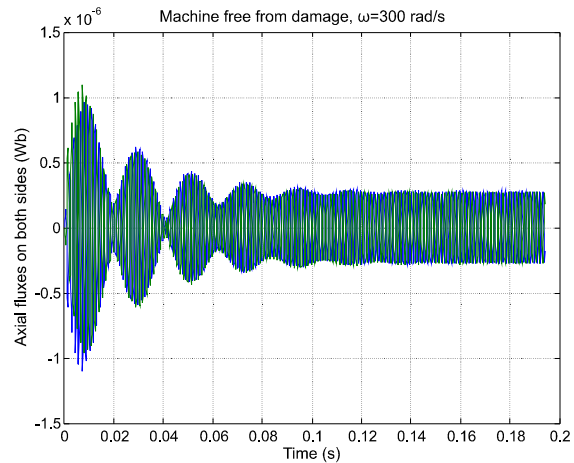

Fig. 4. Very insignificant axial flux in the machine free from damage following switching on at speed of 300 rad/s
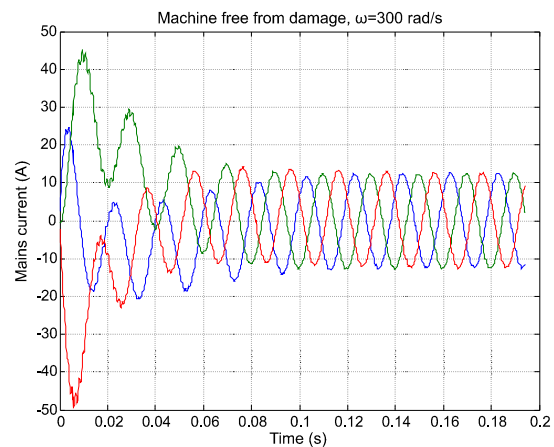

Fig. 5. Mains current in the asynchronous squirrel cage machine free from damage following switching on at speed of 300 rad/s
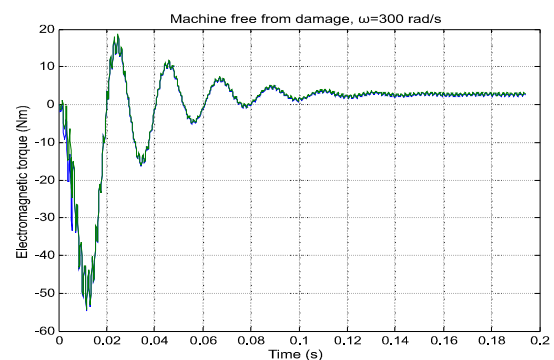

Fig. 6. Electromagnetic torque of the machine free from damage, as calculated for the layer adjacent to the stator and rotor (the results correspond with each other) following switching on at the speed of 300 rad/s

Figures 4 through 6 show the behaviour of the machine free from damage at higher speed of ω=300 rad/s. They show that there is a very minor axial flux magnitude. In contrast, when a ring segment is damaged, the axial flux increases, but its pulsation would be minor, i.e. of 14,15 rad/s. It would require long computations to get the precise time-domain courses. So to consider this phenomenon, calculations were made at ω=100 rad/s for the machine with fractured ring. The results are shown in Figs. 8 through 10. To compare the magnitudes of axial fluxes which develop in the machine free from damage, Figure 7 was included showing the time-domain courses at 60 rad/s.
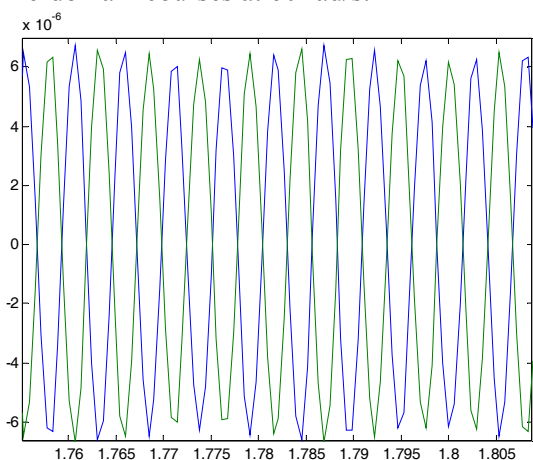

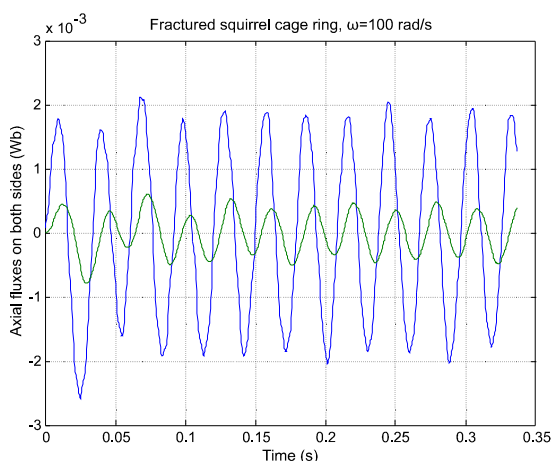Fig. 7. *Axial fluxes in the machine free from damage at speed of 60 rad/s*

Fig. 8. *Axial flux on both sides of the squirrel cage at fractured squirrel cage ring and speed of 100 rad/s*
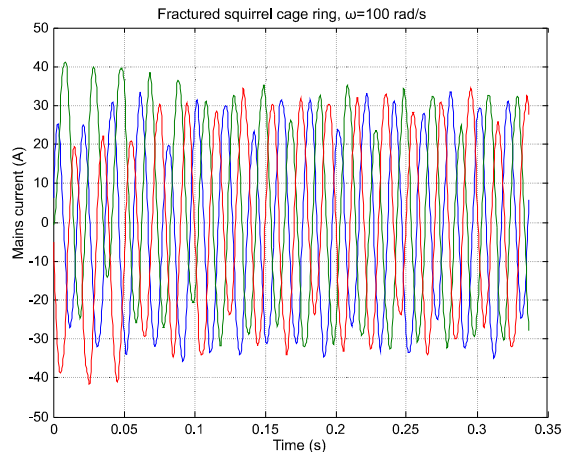

Fig. 9. *Mains current at fractured squirrel cage ring and speed of 100 rad/s*
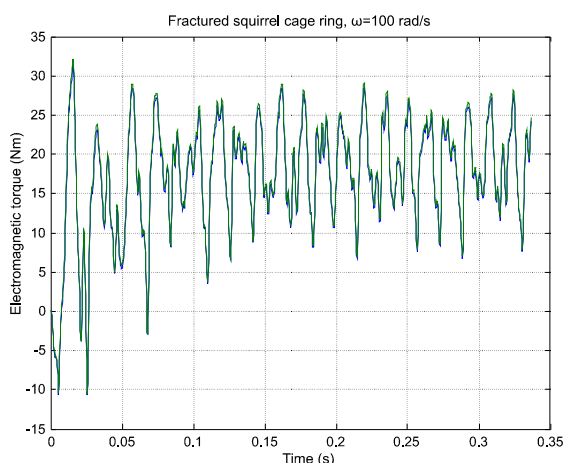

Fig. 10. *Electromagnetic torque of the defective machine with fractured ring, as calculated for the layer adjacent to the stator and rotor (the results correspond with each other) following switching on at the speed of 100 rad/s*

The axial flux increases due to some deteriorated inter-laminar insulation in the stator e.g. in the range of one slot pitch. The stator laminated stack damaged in such manner, may generate voltage in the shaft of the machine, and voltage between the sides of the laminated stator stack in the area of damaged insulation, increase axial flux in both shaft ends by the same value. This was shown by comparing a machine free from damage with one of damaged laminated stack versus speed in Fig. 11.
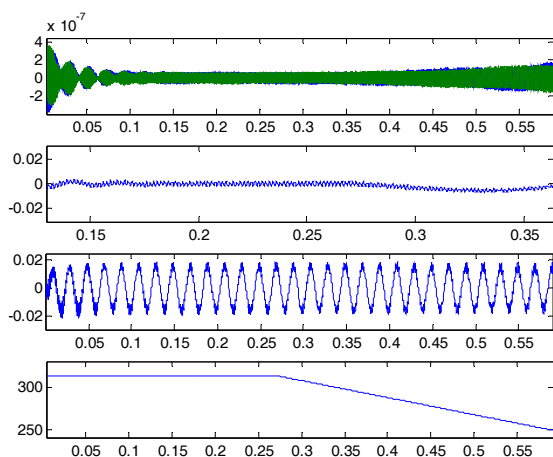
Fig. 11. Machine free from damage, a) axial fluxes, b) shaft voltage, c) voltages between sides of laminated stator stacks, d) assumed speed step
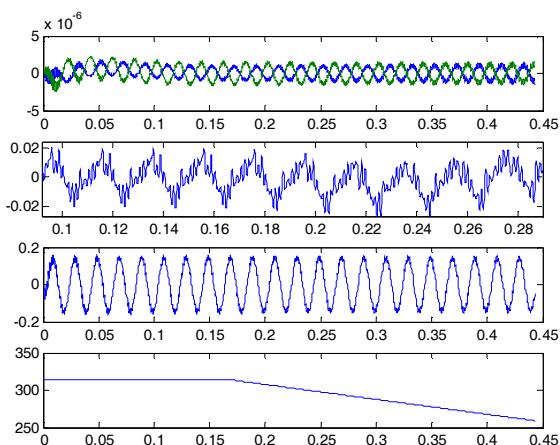

Fig.12 Damaged machine, a) axial fluxes, b) shaft voltage, c) voltages between sides of laminated stator stacks in the area of damaged inter-laminar insulation, d) assumed speed step

The following numerical remarks can be made, based on the calculation results. The axial flux exhibits minor susceptibility to the deformation of the elements found in the airgap of the machine during rotation of the rotor. In contrast, the electromagnetic torque as calculated by Coulomb method as well as the forces acting on the rotor, are susceptible to this deformation. So to get more accurate calculations of the torque, it is necessary to increase the number of elements in the airgap of the machine. The electromagnetic torque in the layer found at the machine rotor, which does not deform at rotation, exhibits higher computational stability.

To conform the results of calculations obtained in the process of calculations, experimental research has been conducted for the motor of out-put of 50 kW, 1500 rpm. Fig. 13 shows the shaft-coil voltages in the machine free from damage a) as well as with fractured ring segment b). The time-domain courses show high susceptibility of the axial flux to ring damage. Both the shaft-coil voltage magnitudes shown in Fig. 13 as well as the main pulsation, support the results obtained from the calculations for the axial flux.
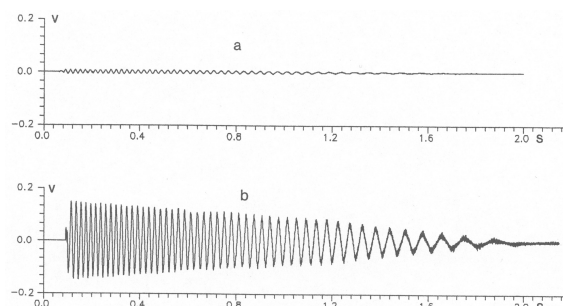

Fig. 13. The measured voltage of one shaft-coil: a) machine free from damage, b) crack of ring of cage

4. Conclusions

The numerical calculations as conducted by 3D FEM program, have confirmed the conclusions drawn from the theoretical studies [4], [6] as far the development of the axial flux in the electric machine is concerned. They also demonstrated how effective is the developed program at studying the dynamic properties of the electric machine. One can also notice that:

1) Both the magnitude and the specifics of the voltage induced by the axial flux, in the diagnostic coil located around the rotor shaft, depend on the damage location and its type.
2) Method of monitoring the axial flux level is particularly useful at detecting defects in the 3-phase windings (e.g. winding short circuiting) as well as damage to the rings of the squirrel cages of rotors of the induction and asynchronous machines.
3) The squirrel cage bar fracture is difficult to detect by merely monitoring the axial flux.

The axial flux properties, as discussed above, made it a very useful parameter at diagnostics of the rotating alternating-current machines, as a simple coil of few to few tens turns put over the shaft of the machine will suffice to detect its occurrence. The magnitude as well as the type of the voltage induced in the coil by the axial flux, depend on both the location and size of the damage to the machine circuitry.

There are numerous phenomena in the induction machine, which require 3D calculations. Axial flux is a good example here. At the same time there is no chance to use any symmetry of such phenomenon and conduct calculations only in some part of the machine. The program presented here by the authors, is able to take into account the detailed form of the machine, including stator laminated stack, rotor laminated stack, windings, housing and the bearing area. The program is able to conduct calculations for transient states of the machine. It is very easy to simulate any damage of the machine, which was shown for the case of fractured bar, fractured ring, and damaged laminated stator stack. The program takes into account non-linear iron magnetisation characteristic. By assuming the magnetic permeability tensor of υ, one can take into account magnetic asymmetry of laminated stator and rotor stacks. By summing electric permeability tensor for the laminated stacks, bars and rings, it is possible to simulate stator eddy currents, rotor cross currents, and the squirrel cage itself. Application of finite elements as shown in Fig. 2 made it possible to simulate rotor squirrel skew.

For example, for the case of 36 stator teeth and 28 rotor squirrel cage bars with skew, the total number of unknowns was 1951811, including 176986 nodes with unknown scalar potential. The tetrahedral number was 1439524. There were total of 272430 nodes. The number of non-zero elements of sparse matrix of the system was 39444439. At unoptimised usage of operating memory the Matlab system, including the program itself, used up some 2Gb. Rotor teeth skew is one of the methods of limiting the voltage magnitude in the motor shaft.

5. References

[1]. Albertz D., Henneberger G.: On the use of the new edge based A-A, T formulation for the calculation of time-harmonic, stationary and transient eddy current field problems, IEEE Transactions on Magnetics vol. 36, no. 4, July 2000, pp 818-822.

[2]. De Gersem H., Gyselinck J. J. C., Dular P., Hameyer K., Weiland T.: Comparison of sliding-surface and moving-band techniques in frequency-domain finite-element models of rotating machines, COMPEL, vol. 23 no. 3, 2004, pp. 1007-1014.

[3]. Ramesohl L., Henneberger G., Küppers S., Hadrys W.: *Three dimensional calculation of magnetic forces and displacements of a claw-pole generator*, IEEE Transactions on Magnetics vol. 32, no. 3, 1996, pp 1685-1688.

[4]. Dziwniel P., Boualem B., Piriou F., Ducreux J.-P., Thomas P.: *Comparison between two approaches to model induction machines with skewed slots*, IEEE Transactions on Magnetics vol. 36, no. 4, 2000, pp 1453-1457.

[5]. Dziwniel P., Piriou F., Ducreux J.-P., Thomas P.: *A time-stepped 2D-3D finite element method for induction motors with skewed slots modelling*, IEEE Transactions on Magnetics vol. 35, no. 3, 1999, pp 1262-1265.

[6]. Xin Xie, Pan G., Hall S.: *A Crank-Nicholson-based unconditionally stable time domain algorithm for 2D and 3D problems*, Microwave and Optical Technology Letters, Vol. 49, No. 2, February 2007.

[7]. Jin J. M.: *The Finite Element Method in Electromagnetics* (2nd Edition), John Wiley & Sons, New York 2002.

[8]. Hausberg V., Seinsch H. O.: *Wellenspannungen und zirkulierende Lagerstrome bei umrichtergespeisten Induktionmaschinen*, Electrical Engineering 82 (2000), Springer-Verlag 2000, pp. 313-326.

[9]. Gersem H., Hameyer K., Weiland T.: *Field_circuit coupled models in electromagnetic simulation*, Journal of Computational and Applied Mathematics, No. 168 (2004), pp 125-133.

[10]. Sande H. V., Boonen T., Podoleanu I., Henrotte F., Hameyer K.: *Simulation of a Three-Phase Transformer Using an Improved Anisotropy Model*, IEEE Transactions on Magnetics, vol. 40, no. 2, March 2004.

Authors

Marian Noga – Akademia Górniczo-Hutnicza, Wydział Elektrotechniki, Automatyki, Informatyki i Elektroniki, Katedra Automatyki Napędu i Urządzeń Przemysłowych, Kraków, al. Mickiewicza 30, B-1/120a
e-mail: manoga@cyfronet.krakow.pl.

Lesław Gołębiowski, Marek Gołębiowski, Damian Mazur is with the Rzeszow Institute of Technology, Electric and Information Technology Department, ul. W. Pola 2, B209, 35-959 Rzeszów, Poland,
(e-mail: golebiye@prz.rzeszow.pl,
        yegolebi@prz.rzeszow.pl,
        mazur@prz.rzeszow.pl).